

See discussions, stats, and author profiles for this publication at: <https://www.researchgate.net/publication/264259156>

# Synthesis and Characterization of Gold Clusters Ligated with 1,3-Bis(dicyclohexylphosphino)propane

ARTICLE *in* CHEMPLUSCHEM · SEPTEMBER 2013

Impact Factor: 3 · DOI: 10.1002/cplu.201300134

---

CITATIONS

5

---

READS

9

3 AUTHORS, INCLUDING:



**Grant Johnson**

Pacific Northwest National Laboratory

44 PUBLICATIONS 987 CITATIONS

SEE PROFILE



**Julia Laskin**

Pacific Northwest National Laboratory

209 PUBLICATIONS 4,783 CITATIONS

SEE PROFILE



# Synthesis and Characterization of Gold Clusters Ligated with 1,3-Bis(dicyclohexylphosphino)propane

Grant E. Johnson,\* Thomas Priest, and Julia Laskin<sup>[a]</sup>

*In memory of Detlef Schröder*

In this multidisciplinary study the chemical reduction synthesis of novel gold clusters in solution was combined with high-resolution analytical mass spectrometry (MS) to gain insight into the composition of the gold clusters and how their size, ionic charge state, and ligand substitution influences their gas-phase fragmentation pathways. Ultrasmall cationic gold clusters ligated with 1,3-bis(dicyclohexylphosphino)propane (dcp) were synthesized for the first time and introduced into the gas phase using electrospray ionization (ESI). Mass-selected cluster ions were fragmented by employing collision-induced dissociation (CID) and the product ions were analyzed using MS. The solutions were found to contain the multiply charged cationic gold clusters  $\text{Au}_9\text{L}_4^{3+}$ ,  $\text{Au}_{13}\text{L}_5^{3+}$ ,  $\text{Au}_6\text{L}_3^{2+}$ ,  $\text{Au}_8\text{L}_3^{2+}$ , and  $\text{Au}_{10}\text{L}_4^{2+}$  ( $\text{L}=\text{dcp}$ ). The gas-phase fragmentation pathways of these cluster ions were examined systematically by employing CID combined with MS. In addition, CID experiments were per-

formed on related gold clusters of the same size and ionic charge state but capped with 1,3-bis(diphenylphosphino)propane (dppp) ligands containing phenyl functional groups at the two phosphine centers instead of cyclohexane rings. It is shown that this relatively small change in the molecular substitution of the two phosphine centers in diphosphine ligands ( $\text{C}_6\text{H}_{11}$  versus  $\text{C}_6\text{H}_5$ ) exerts a pronounced influence on the size of the species that are preferentially formed in solution during reduction synthesis as well as the gas-phase fragmentation channels of otherwise identical gold cluster ions. The mass spectrometry results indicate that in addition to the length of the alkyl chain between the two phosphine centers, the substituents at the phosphine centers also play a crucial role in determining the composition, size, and stability of diphosphine-ligated gold clusters synthesized in solution.

## Introduction

The scalable solution-phase synthesis of clusters containing an exact number of metal atoms and capping ligands has remained a topic of considerable interest owing to the potential applications of these nanomaterials in a wide range of future technologies.<sup>[1]</sup> For example, the highly size-dependent chemical and physical properties of nanoscale gold clusters make them particularly amenable for use in heterogeneous catalysis,<sup>[2]</sup> nanoscale electronics,<sup>[3]</sup> molecular threat detection,<sup>[4]</sup> biomedicine,<sup>[3b–5]</sup> and cluster-assembled materials.<sup>[6]</sup> In general, size selectivity is achieved in solution-phase reduction synthesis through the use of various capping ligands such as phosphines,<sup>[7]</sup> diphosphines,<sup>[8]</sup> and thiols.<sup>[9]</sup> When employed under carefully optimized reaction conditions these ligands may arrest the growth of small gold clusters at specific sizes and achieve relatively tight control over the final distribution of cluster sizes present in solution.<sup>[9a]</sup> Nevertheless, it is often the case that additional purification procedures such as polyacrylamide gel electrophoresis (PAGE),<sup>[10]</sup> fractional precipitation,<sup>[11]</sup>

hydrodynamic fractionation,<sup>[12]</sup> or size-exclusion chromatography<sup>[13]</sup> are necessary to prepare completely monodisperse cluster distributions through reduction synthesis in solution.

Over the last few years, diphosphine ligands have received increasing attention owing to their reported ability to stabilize monodisperse cationic gold clusters of specific sizes in solution.<sup>[8d–14]</sup> The study by Bertino and co-workers demonstrated that bidentate phenyl-substituted diphosphine ligands are capable of producing monodisperse triply charged cationic  $\text{Au}_{11}$  clusters if the alkyl chain between the two phosphine groups of the ligand is three carbon atoms long.<sup>[15]</sup> In addition, they showed that for diphosphine ligands containing longer alkyl chains of five and six carbon atoms the preferred sizes of clusters produced in solution are  $\text{Au}_{10}$  and  $\text{Au}_8$ , respectively. Further studies by Bergeron and co-workers examined the synthesis and fragmentation pathways of small cationic  $\text{Au}_8$ ,  $\text{Au}_{10}$ , and  $\text{Au}_{11}$  clusters prepared by employing both 1,3-bis(diphenylphosphino)propane (dppp) and 1,5-bis(diphenylphosphino)pentane.<sup>[16]</sup> Collision-induced dissociation (CID) experiments showed loss of a neutral ligand as well as  $\text{AuL}^+$  and  $\text{Au}_3\text{L}^+$  ( $\text{L}=\text{ligand}$ ) from the precursor ion to be common fragmentation pathways for these clusters. In a subsequent publication the same authors examined the initial ligand-exchange reactions in solution, which produce the critical intermediates that are the precursors to the formation of larger gold clusters.<sup>[17]</sup> A related study by Pettibone and co-workers has shown that by

[a] Dr. G. E. Johnson, T. Priest, Dr. J. Laskin  
Physical Sciences Division  
Pacific Northwest National Laboratory  
P.O. Box 999, MSIN K8-88  
Richland, WA 99352 (USA)  
E-mail: Grant.Johnson@pnnl.gov

Supporting information for this article is available on the WWW under <http://dx.doi.org/10.1002/cplu.201300134>.

varying the ratio of the diphosphine ligand to triphenylphosphine in the initial reaction mixtures it is possible to control the size of the resulting gold clusters in the range of  $\text{Au}_8$  to  $\text{Au}_{10}$ .<sup>[8d]</sup> In another publication the same authors investigated the different types of complexes that form initially between diphosphine ligands and gold atoms in solution. This study examined diphosphine ligands with alkyl chains containing one to six carbon atoms.<sup>[18]</sup> By using mass spectrometry they were able to track the evolution of different types of initial metal complexes into larger gold clusters. In a similar vein, detailed reaction pathways for the production of larger gold clusters from smaller clusters and the metal–ligand complexes that are formed initially in solution have been proposed for 1,5-bis(diphenylphosphino)pentane.<sup>[8b]</sup>

It is currently well established that diphosphine ligands are capable of controlling the growth of cationic gold clusters during reduction synthesis in solution. The origin of the size selectivity and how it depends on the properties of different diphosphine ligands (length of the alkyl chain between the phosphine centers and substitution of the phosphine centers), however, remains a subject of active research. In a recent publication, Hong and co-workers employed density functional theory (DFT) to examine the reactivity and selectivity of simplified model diphosphine ligands with the formula  $\text{PH}_2(\text{CH}_2)_m\text{PH}_2$  (spacer  $m=3, 5$ ) toward cationic  $\text{Au}_n$  ( $n=7-11$ ) clusters.<sup>[19]</sup> Their findings indicate that the shorter diphosphine ligand, which contains three  $\text{CH}_2$  spacer units, is far less flexible than the longer ligand that contains five  $\text{CH}_2$  units. They propose that this lack of geometrical flexibility of the shorter alkyl chain necessitates a much larger input of energy for the shorter ligand to flex sufficiently to coordinate gold cores of different sizes. Therefore, the shorter ligand will only stabilize gold clusters in a narrow size range that does not require excessive flexing of the relatively stiff alkyl chain. In comparison, the longer diphosphine ligand may flex much more easily to accommodate gold cores of different sizes.<sup>[19]</sup> These calculations, along with others in the literature, make use of a simplified model diphosphine ligand in which the two computationally demanding phenyl groups at each phosphine center have been replaced by much simpler hydrogen atoms ( $\text{C}_6\text{H}_5 \rightarrow \text{H}$ ). This is a common practice in the modeling of ligated clusters and it is generally assumed that the substitution at the phosphine centers does not significantly influence the reactive properties of the overall diphosphine ligand. There is, however, both experimental and theoretical evidence that this assumption may not be valid in all situations. For example, cationic gold clusters capped with the ethyl-substituted diphosphine ligand 1,3-bis(diethylphosphino)propane (depp) have been synthesized and it was found that substitution of ethyl for phenyl groups at the phosphine centers results in drastically different compositions and charge states of the gold clusters prepared in solution at similar conditions.<sup>[20]</sup> Indeed, it was proposed that the ethyl groups increase the electron-donating properties of the phosphine centers and cause charge to transfer from the ligands to the gold core. This increased charge density on the gold core results in the preferential formation of the singly charged chlorinated gold clusters  $\text{Au}_{11}\text{L}_4\text{Cl}_2^+$ ,  $\text{Au}_{12}\text{L}_4\text{Cl}_3^+$ , and  $\text{Au}_{13}\text{L}_4\text{Cl}_4^+$

in solution instead of  $\text{Au}_{11}\text{L}_5^{3+}$ , which is formed with the phenyl-substituted ligand. These results indicate that in addition to the length of the alkyl spacer of diphosphine ligands, the functional groups at the phosphine centers also play a critical role in determining the cluster size, charge state, and composition.

Herein, we report the chemical reduction synthesis of novel subnanometer gold clusters capped with dcpp and their characterization using high-resolution analytical mass spectrometry. We demonstrate that a simple substitution of the aromatic phenyl ring with the saturated cyclohexane moiety at the phosphine centers of the diphosphine ligands has a pronounced effect on the species that are formed preferentially in solution as well as the gas-phase fragmentation pathways of otherwise identical gold cluster ions. The results show how the substituents at the phosphine centers of diphosphine ligands ( $\text{C}_6\text{H}_{11}$  versus  $\text{C}_6\text{H}_5$ ) control the preferred size and ionic charge state of gold clusters synthesized in solution. Moreover, CID experiments provide insight into how size and ionic charge state influence the gas-phase fragmentation pathways of novel dcpp-capped gold clusters.

## Results and Discussion

Subnanometer cationic gold clusters ligated with dcpp were synthesized in solution and subsequently analyzed using ESI-MS and CID. The synthesis procedure used in the present study for clusters capped with dcpp is essentially identical to a procedure reported in the literature for clusters capped with dppp with the substitution of the strong reducing agent, sodium borohydride, in place of the weaker reducing agent, the borane *tert*-butylamine complex.<sup>[16]</sup> The most obvious difference between the two procedures is that gold cluster formation with dppp ligands using borane *tert*-butylamine as the reducing agent occurred much more rapidly ( $\approx 3$  h) than the synthesis with dcpp ligands using sodium borohydride, which took approximately 3 days. A representative mass spectrum of cationic gold clusters ligated with dcpp is presented in Figure 1a. The triply charged  $\text{Au}_9\text{L}_4^{3+}$  ( $m/z$  1173.02) cluster is the dominant ion in the mass spectrum followed by another less abundant triply charged cluster,  $\text{Au}_{13}\text{L}_5^{3+}$  ( $m/z$  1581.09). Less abundant doubly charged gold clusters, including  $\text{Au}_7\text{L}_2^{2+}$  ( $m/z$  633.31),  $\text{Au}_6\text{L}_3^{2+}$  ( $m/z$  1245.41),  $\text{Au}_8\text{L}_3^{2+}$  ( $m/z$  1442.32), and  $\text{Au}_{10}\text{L}_4^{2+}$  ( $m/z$  1858.01) were also observed in the mass spectrum under mild source conditions that minimize in-source fragmentation. These results demonstrate, for the first time, the size-selective synthesis of novel subnanometer cationic gold clusters using the cyclohexane-substituted diphosphine ligand dcpp.

The dcpp ligand, which contains two coordinating phosphine groups that are separated by an alkyl chain of three carbon atoms, is similar in structure and composition to the phenyl-substituted dppp ligand, which has been reported previously to exclusively stabilize  $\text{Au}_{11}\text{L}_5^{3+}$  ( $\text{L}=\text{dppp}$ ) in solution.<sup>[15,16]</sup> A representative mass spectrum of gold clusters stabilized by dppp obtained by using identical instrumental conditions is presented in Figure 1b for comparison. In agreement

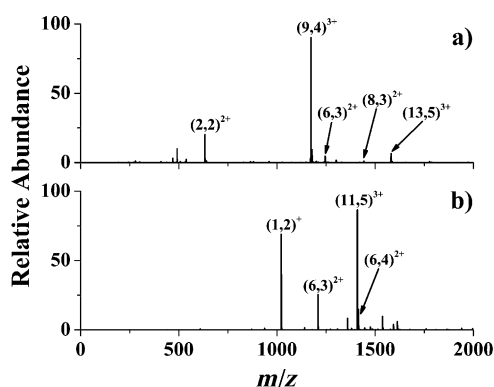


**Figure 1.** Representative positive-mode electrospray mass spectra of solutions of gold clusters capped with (a) 1,3-bis(dicyclohexylphosphino)propane (dcpp) and (b) 1,3-bis(diphenylphosphino)propane (dppp) in methanol. The bracket notation ( $x, y$ ) indicates the number of Au atoms and dcpp or dppp ligands in the cluster, respectively.

with previously reported ESI-MS characterization of gold clusters stabilized by dppp,  $\text{Au}_{11}\text{L}_5^{3+}$  appears as the dominant ion in the mass spectrum owing to its highly stable eight-electron closed-shell electronic structure.<sup>[21]</sup> Interestingly, this cluster is not observed when dcpp is used as the ligand (Figure 1a). In contrast, less abundant doubly charged cluster species including  $\text{Au}_6\text{L}_3^{2+}$  and  $\text{Au}_{10}\text{L}_4^{2+}$  are observed with both ligands, whereas  $\text{Au}_6\text{L}_4^{2+}$  ( $m/z$  1415.70) is present only in solution containing dppp-capped gold clusters. The dcpp ligand used in the current study also shares the same length of carbon backbone as the related ethyl-substituted depp ligand that has been used previously to synthesize small singly charged chlorinated gold clusters including  $\text{Au}_{11}\text{L}_4\text{Cl}_2^+$  ( $m/z$  3117.17),  $\text{Au}_{12}\text{L}_4\text{Cl}_3^+$  ( $m/z$  3351.11), and  $\text{Au}_{13}\text{L}_4\text{Cl}_4^+$  ( $m/z$  3583.04).<sup>[20]</sup> These previous studies of gold clusters capped with dppp and depp, combined with our current findings for dcpp-ligated gold clusters, indicate that by changing the four substituents at the two phosphine centers of diphosphine ligands while keeping the length of the alkyl chain constant, it is possible to dramatically influence the size, composition, and ionic charge state of cationic gold clusters formed through reduction synthesis in solution (dcpp =  $\text{Au}_9\text{L}_4^{3+}$ , dppp =  $\text{Au}_{11}\text{L}_5^{3+}$ , depp =  $\text{Au}_{11}\text{L}_4\text{Cl}_2^+$ ).

In an earlier publication, Golightly and co-workers attributed the difference in composition and ionic charge state of gold clusters stabilized with dppp versus depp to changes in the relative electron-withdrawing and -donating abilities of the two phosphine centers, which depends on their substitution.<sup>[20]</sup> Specifically, they proposed that phenyl-substituted dppp has electron-withdrawing properties and ethyl-substituted depp has a tendency to force charge density onto the central core of the gold clusters. The increased charging of the gold core resulting from ligation by depp necessitates the presence of two electron-withdrawing Cl groups to achieve the energetically preferred 3+ charge state of the gold core. This results in the preferential formation of singly charged  $\text{Au}_{11}\text{L}_4\text{Cl}_2^+$  for depp and triply charged  $\text{Au}_{11}\text{L}_5^{3+}$  for dppp.<sup>[20]</sup> Our current findings for cationic gold clusters ligated with cyclohexane-substituted dcpp presented in Figure 1a do not indicate the pres-

ence of any chlorinated gold species similar to what was observed previously for depp-capped clusters.

As alluded to earlier, the large abundance of  $\text{Au}_{11}\text{L}_5^{3+}$  ( $\text{L} = \text{dppp}$ ) observed in solution has been previously attributed to the exceptional stability of this cluster, which results from a closed electronic shell of eight electrons ( $11 - 3 = 8$ ), thereby suggesting spherical cluster geometry (shell closings at 2, 8, 18, 34, 58, etc.).<sup>[15–22]</sup> In comparison,  $\text{Au}_9\text{L}_4^{3+}$  ( $\text{L} = \text{dcpp}$ ), which contains six electrons from the gold atoms, does not satisfy the shell-closing requirement for a spherical 3D cluster. Instead, the large abundance of this cluster may be justified as resulting from a stable closed shell of six electrons ( $9 - 3 = 6$ ) suggesting that the cluster has a 2D ellipsoidal (shell closings at 2, 6, 12, 20, 30, etc.) instead of a 3D spherical geometry.<sup>[23]</sup> Why substitution of cyclohexane in place of phenyl in an otherwise identical diphosphine ligand results in a transition from a 3D spherical to a 2D ellipsoidal geometry of the gold clusters is not readily apparent. Recently, structural calculations were employed to address the influence of the length of the alkyl chain that separates the phosphine centers on the selectivity of diphosphine ligands towards different sizes of gold clusters.<sup>[19]</sup> We propose that a similar effort to better understand the influence of different substituents at the two phosphine centers may also be extremely fruitful.

To investigate how size (number of gold atoms and dcpp ligands) influences the fragmentation behavior of novel triply charged cationic gold clusters capped with dcpp we isolated both  $\text{Au}_9\text{L}_4^{3+}$  and  $\text{Au}_{13}\text{L}_5^{3+}$  and subjected them to CID by employing argon gas as a neutral collision partner. The mass spectra of the fragment ions produced through CID of these triply charged gold clusters are presented in Figure 2. A complete

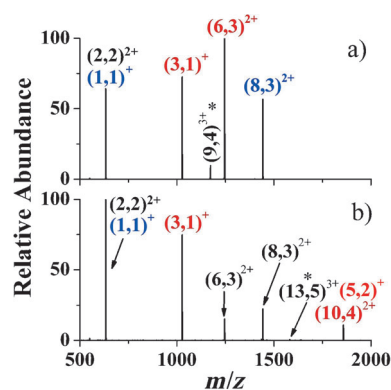


**Figure 2.** CID spectra of (a)  $\text{Au}_9\text{L}_4^{3+}$  and (b)  $\text{Au}_{13}\text{L}_5^{3+}$  ( $\text{L} = \text{dcpp}$ ) cluster ions. The isolated precursor ions are highlighted with an asterisk. The colors identify complementary fragments.

list of fragment ions observed for  $\text{Au}_9\text{L}_4^{3+}$  is presented in Table S1 in the Supporting Information. The smaller  $\text{Au}_9\text{L}_4^{3+}$  cluster dissociates into two sets of complementary fragment ions that are color coded as blue and red in Figure 2a. The dominant fragment is doubly charged  $\text{Au}_6\text{L}_3^{2+}$  followed by its singly charged complementary ion  $\text{Au}_3\text{L}^+$ . The second set of complementary fragments,  $\text{AuL}^+$  and  $\text{Au}_8\text{L}_3^{2+}$ , are almost equal in abundance. Therefore, the major dissociation path-

ways of the smaller  $\text{Au}_9\text{L}_4^{3+}$  cluster are surprisingly simple. Both sets of complementary ions have a smaller ion with a single charge ( $\text{AuL}^+$  and  $\text{Au}_3\text{L}^+$ ) and a larger ion carrying two charges ( $\text{Au}_6\text{L}_3^{2+}$  and  $\text{Au}_8\text{L}_3^{2+}$ ). No fragments corresponding to the loss of neutral ligands or gold atoms from the triply charged precursor ion are observed. Table S1 also shows that some minor fragments resulting from dissociation of the dcpp ligands are present in the CID spectrum of  $\text{Au}_9\text{L}_4^{3+}$ . Both of the major doubly charged primary fragment ions,  $\text{Au}_6\text{L}_3^{2+}$  and  $\text{Au}_8\text{L}_3^{2+}$ , exhibit minor secondary dissociation products resulting from loss of  $\text{C}_6\text{H}_{11}$  units forming  $\text{Au}_x\text{L}_3-(\text{C}_6\text{H}_{11})_y^{2+}$  ( $x=6, 8$ ;  $y=1, 2$ ). Analogous secondary product ions resulting from the loss of  $\text{C}_6\text{H}_{11}$  from  $\text{AuL}^+$  forming  $\text{AuL}-(\text{C}_6\text{H}_{11})_x$  ( $x=1, 2$ ) are also observed for  $\text{Au}_9\text{L}_4^{3+}$ .

Similarly to  $\text{Au}_9\text{L}_4^{3+}$ , the larger  $\text{Au}_{13}\text{L}_5^{3+}$  cluster dissociates to produce abundant  $\text{AuL}^+$  and  $\text{Au}_3\text{L}^+$  fragments accompanied by the corresponding doubly charged complementary ions,  $\text{Au}_{12}\text{L}_4^{2+}$  and  $\text{Au}_{10}\text{L}_4^{2+}$ , which appear with much lower relative abundance in the CID spectrum in Figure 2b. In addition to the most abundant complementary fragment ions described above, two doubly charged product ions,  $\text{Au}_6\text{L}_3^{2+}$  and  $\text{Au}_8\text{L}_3^{2+}$ , are observed in the CID spectrum of the  $\text{Au}_{13}\text{L}_5^{3+}$  cluster. Upon closer inspection, extremely minor peaks corresponding to the complementary fragments  $\text{Au}_7\text{L}_2^+$  and  $\text{Au}_5\text{L}_2^+$  are also observed but cannot be seen in Figure 2b. In addition, through high-resolution mass spectrometry, it is also possible to discern the presence of both a major  $\text{AuL}^+$  and minor  $\text{Au}_2\text{L}_2^{2+}$  fragment ion at  $m/z$  633.3045 through the spacing between the individual isotopes in the overall isotopic envelope of the species. A complete list of CID fragments observed for  $\text{Au}_{13}\text{L}_5^{3+}$  is presented in Table S1. In comparison with the smaller  $\text{Au}_9\text{L}_4^{3+}$ , the larger  $\text{Au}_{13}\text{L}_5^{3+}$  cluster exhibits fewer minor secondary fragment ions corresponding to the loss of  $\text{C}_6\text{H}_{11}$  from the primary dissociation products. Nevertheless, the  $\text{Au}_6\text{L}_3^{2+}$  and  $\text{AuL}^+$  product ions exhibit the same loss of  $\text{C}_6\text{H}_{11}$  for both  $\text{Au}_9\text{L}_4^{3+}$  and  $\text{Au}_{13}\text{L}_5^{3+}$  primary ions. A minor peak corresponding to the loss of a neutral dcpp ligand from  $\text{Au}_{13}\text{L}_5^{3+}$  forming  $\text{Au}_{13}\text{L}_4^{3+}$  is also observed in Table S1.

The results presented in Figure 2 for  $\text{Au}_9\text{L}_4^{3+}$  and  $\text{Au}_{13}\text{L}_5^{3+}$  capped with dcpp share some similarity to the findings of CID experiments conducted previously on the triply charged  $\text{Au}_{11}\text{L}_5^{3+}$  cluster ligated with dppp.<sup>[16–24]</sup> Specifically, experiments by Bergeron and co-workers demonstrated singly charged  $\text{AuL}^+$  ( $\text{L}=\text{dppp}$ ) to be the dominant CID fragment along with the complementary doubly charged  $\text{Au}_{10}\text{L}_4^{2+}$  ion. A second, less abundant set of complementary fragment ions,  $\text{Au}_3\text{L}^+$  and  $\text{Au}_8\text{L}_4^{2+}$ , was also observed.<sup>[16]</sup> The results of Bergeron and co-workers agree qualitatively with the more recent study by Robinson and co-workers, which found loss of a neutral ligand from  $\text{Au}_{11}\text{L}_5^{3+}$  ( $\text{L}=\text{dppp}$ ) forming  $\text{Au}_{11}\text{L}_4^{3+}$  to be an additional minor fragmentation channel.<sup>[24]</sup> Therefore, triply charged cationic gold clusters ligated with dcpp and dppp share some similar fragmentation pathways that produce small singly charged  $\text{AuL}^+$  and  $\text{Au}_3\text{L}^+$  ions along with the larger doubly charged complementary ions. In comparison with  $\text{Au}_{11}\text{L}_5^{3+}$  ( $\text{L}=\text{dppp}$ ), the smaller  $\text{Au}_9\text{L}_4^{3+}$  ( $\text{L}=\text{dcpp}$ ) does not show any loss of a neutral ligand from the precursor ion. As

mentioned above,  $\text{Au}_{13}\text{L}_5^{3+}$  ( $\text{L}=\text{dcpp}$ ) does exhibit loss of one ligand to form  $\text{Au}_{13}\text{L}_4^{3+}$  but only as an extremely minor channel. Partial loss of a ligand  $-\text{P}(\text{C}_6\text{H}_5)_3$  from  $\text{Au}_{11}\text{L}_5^{3+}$  ( $\text{L}=\text{dppp}$ ) forming  $\text{Au}_{11}\text{L}_4(\text{C}_6\text{H}_5)\text{P}(\text{CH}_2)_3^{3+}$  was observed previously by Bergeron and co-workers. These earlier results combined with our current findings indicate that activation of dppp as well as dcpp ligands is possible during gas-phase CID experiments on triply charged gold clusters.<sup>[16]</sup> However, activation of dcpp occurs primarily through sequential loss of  $\text{C}_6\text{H}_{11}$  units, whereas activation of dppp involves the removal of an entire phosphine group.

In addition to size, the ionic charge state of dcpp-capped cationic gold clusters has the potential to influence their gas-phase stability and fragmentation pathways. To facilitate a comparison between the properties of triply and doubly charged gold clusters, as well as doubly charged clusters of different size, CID experiments were conducted on doubly charged  $\text{Au}_6\text{L}_3^{2+}$ ,  $\text{Au}_8\text{L}_3^{2+}$ , and  $\text{Au}_{10}\text{L}_4^{2+}$  ( $\text{L}=\text{dcpp}$ ) clusters. As shown in Figure 3a, the smallest doubly charged  $\text{Au}_6\text{L}_3^{2+}$  cluster undergoes dissociation to form two sets of singly charged comple-

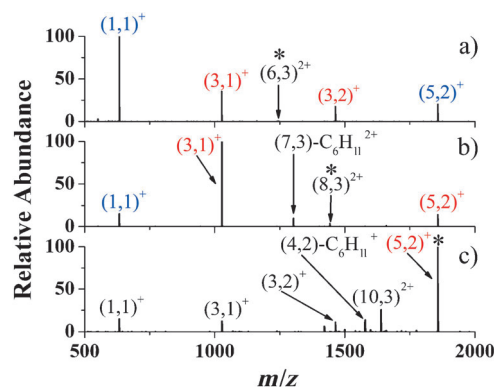


**Figure 3.** CID spectra of (a)  $\text{Au}_6\text{L}_3^{2+}$ , (b)  $\text{Au}_8\text{L}_3^{2+}$ , and (c)  $\text{Au}_{10}\text{L}_4^{2+}$  ( $\text{L}=\text{dcpp}$ ) cluster ions. The isolated precursor ions are highlighted with an asterisk. The colors identify complementary fragments.

mentary ions. The  $\text{AuL}^+$  ion is the dominant fragment and appears at much higher relative abundance than its complementary  $\text{Au}_5\text{L}_2^+$  ion. The  $\text{Au}_3\text{L}^+$  and  $\text{Au}_3\text{L}_2^+$  ions appear as a second set of complementary fragments with lower relative abundance. Minor products corresponding to ligand activation and loss of both one and two  $\text{C}_6\text{H}_{11}$  groups from larger primary fragment ions are also observed for  $\text{Au}_6\text{L}_3^{2+}$  and are listed in Table S2. The simple fragmentation spectrum of  $\text{Au}_6\text{L}_3^{2+}$  is qualitatively similar to the result described above for the smallest triply charged  $\text{Au}_9\text{L}_4^{3+}$  cluster with the exception of the different charge states (2+ versus 1+) of the larger fragments of 3+ versus 2+ precursor ions, respectively. To the best of our knowledge, the CID spectrum of the analogous phenyl-substituted  $\text{Au}_6\text{L}_3^{2+}$  ( $\text{L}=\text{dppp}$ ) ion has not been reported in the literature. However, the fragmentation of a closely related  $\text{Au}_6\text{L}_3^{2+}$  cluster ligated with 1,4-bis(diphenylphosphino)butane (dppb), which contains four instead of three carbon atoms in the alkyl chain separating the two phosphine groups, has been investigated.<sup>[24]</sup> The dppb-capped cluster undergoes fragmentation



to produce  $\text{AuL}^+$  and  $\text{Au}_5\text{L}_2^+$  similar to the dcpp ligated cluster shown in Figure 3a.

The CID spectrum of the intermediate-sized  $\text{Au}_8\text{L}_3^{2+}$  cluster, which contains two additional gold atoms, is presented in Figure 3b. Similarly to  $\text{Au}_6\text{L}_3^{2+}$ , the intermediate  $\text{Au}_8\text{L}_3^{2+}$  cluster also dissociates into two sets of complementary fragments with  $\text{AuL}^+$  and  $\text{Au}_3\text{L}^+$  appearing as the smaller singly charged fragments. Owing to the selected mass range of the instrument, only  $\text{Au}_5\text{L}_2^+$  was observed out of the larger complementary fragments. Although  $\text{Au}_6\text{L}_3^{2+}$  and  $\text{Au}_8\text{L}_3^{2+}$  share the common fragment ions  $\text{AuL}^+$  and  $\text{Au}_3\text{L}^+$ , the relative abundance of these product ions is very different depending on the size of the precursor ion. The  $\text{AuL}^+$  ion is the dominant fragment for the smaller  $\text{Au}_6\text{L}_3^{2+}$  cluster, whereas for the larger  $\text{Au}_8\text{L}_3^{2+}$  the  $\text{Au}_3\text{L}^+$  ion is the most abundant species in the spectrum and  $\text{AuL}^+$  appears only as a minor peak. In addition, the intermediate-sized  $\text{Au}_8\text{L}_3^{2+}$  cluster exhibits a minor fragmentation channel corresponding to the loss of neutral  $\text{Au}(\text{C}_6\text{H}_{11})$  from the precursor ion forming  $\text{Au}_7\text{L}_3-(\text{C}_6\text{H}_{11})^{2+}$ . Analogous losses of  $\text{Au}(\text{C}_6\text{H}_5)$  from cationic gold clusters capped with several different-length phenyl-substituted diphosphine ligands were reported previously by Robinson and co-workers.<sup>[24]</sup> There is also a precedent for the formation of closely related  $\text{Au}(\text{C}_6\text{H}_5)^+$  species in the gas phase through ion–molecule reactions between bare gold cations and neutral benzene molecules.<sup>[25]</sup> It should be pointed out, however, that the neutral species that is lost from the precursor ion in the current study is  $\text{Au}(\text{C}_6\text{H}_{11})$  where, presumably, the gold atom has taken the position of a hydrogen atom in the otherwise saturated cyclohexane ring. A complete list of fragments obtained through CID of  $\text{Au}_8\text{L}_3^{2+}$  is presented in Table S2. Again, minor dissociation products corresponding to the loss of  $\text{C}_6\text{H}_{11}$  from larger primary fragment ions are observed for  $\text{Au}_8\text{L}_3^{2+}$ .

The CID spectrum of the largest doubly charged dcpp-capped  $\text{Au}_{10}\text{L}_4^{2+}$  cluster ion examined in this study is presented in Figure 3c. The same small singly charged fragments,  $\text{AuL}^+$  and  $\text{Au}_3\text{L}^+$ , that were observed for  $\text{Au}_6\text{L}_3^{2+}$  and  $\text{Au}_8\text{L}_3^{2+}$  are also observed for  $\text{Au}_{10}\text{L}_4^{2+}$ , albeit with greatly reduced relative abundance. In comparison, the dominant fragment ion is singly charged  $\text{Au}_5\text{L}_2^+$ , which is a symmetrical fragment of  $\text{Au}_{10}\text{L}_4^{2+}$ . Unambiguous identification of the singly charged fragment ion from the doubly charged precursor ion was achieved through comparing the spacing between the individual peaks in the isotopic distributions of the precursor and fragment ions. After symmetrical dissociation into  $\text{Au}_5\text{L}_2^+$ , the second most abundant fragment corresponds to loss of a neutral ligand from  $\text{Au}_{10}\text{L}_4^{2+}$  to form  $\text{Au}_{10}\text{L}_3^{2+}$ . This is the only major loss of a neutral ligand that was observed for any of the dcpp-capped clusters examined in this study. Inspection of Figure 3c also reveals the presence of a pronounced  $(\text{Au}_4\text{L}_2)-\text{C}_6\text{H}_{11}^+$  fragment resulting from the loss of  $\text{AuC}_6\text{H}_{11}$  from the symmetrical  $\text{Au}_5\text{L}_2^+$  primary fragment. A large number of related fragments were observed for  $\text{Au}_{10}\text{L}_4^{2+}$  with much lower abundance. These dissociation products are listed in Table S2. The CID of  $\text{Au}_{10}\text{L}_4^{2+}$  clusters ligated with related phenyl-substituted diphosphine ligands containing five<sup>[16]</sup> as well as three to six<sup>[24]</sup> carbon atoms in the alkyl chain have been reported pre-

viously. In the case of the dppp ligand with a three-carbon-atom chain, which is most similar to the dcpp ligand in our current study,  $\text{Au}_{10}\text{L}_4^{2+}$  ( $\text{L}=\text{dppp}$ ) was shown to fragment by loss of a neutral ligand. In comparison, clusters capped with phenyl-substituted diphosphine ligands containing longer four to six carbon-atom alkyl chains fragment both through loss of a neutral ligand and core fission to produce  $\text{Au}_5\text{L}_3^+$ .<sup>[24]</sup>

To enable a direct comparison of the fragmentation pathways of dcpp- and dppp-ligated cationic gold clusters, we conducted a series of CID experiments on related species of the same size and ionic charge state under identical instrumental conditions. The CID spectra of  $\text{Au}_6\text{L}_3^{2+}$  are presented in Figure 4a,b for  $\text{L}=\text{dcpp}$  and  $\text{dppp}$ , respectively. The spectra indi-

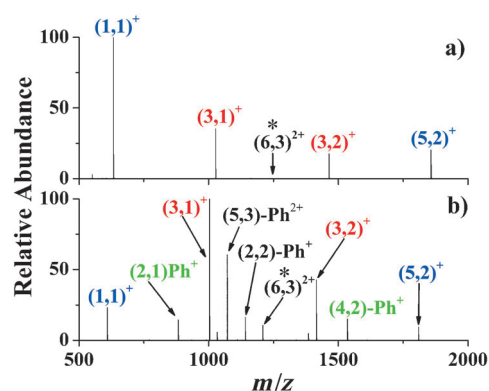


**Figure 4.** CID spectra of  $\text{Au}_6\text{L}_3^{2+}$  for (a)  $\text{L}=\text{dcpp}$  and (b)  $\text{L}=\text{dppp}$ . The isolated precursor ions are highlighted with an asterisk. The colors identify complementary fragments.

cate that substitution of phenyl groups in the place of cyclohexane moieties on an otherwise identical ligand results in the appearance of an additional set of complementary fragments,  $\text{Au}_2\text{L}(\text{C}_6\text{H}_5)^+$  and  $\text{Au}_4\text{L}_2-(\text{C}_6\text{H}_5)^+$ , as well as a peak resulting from the loss of neutral  $\text{Au}(\text{C}_6\text{H}_5)$  from the  $\text{Au}_6\text{L}_3^{2+}$  parent ion forming  $\text{Au}_5\text{L}_3-(\text{C}_6\text{H}_5)^{2+}$ . An additional peak is also observed in Figure 4b that corresponds to  $\text{Au}_2\text{L}_2-(\text{C}_6\text{H}_5)^+$ . A complete list of dissociation products observed for  $\text{Au}_6\text{L}_3^{2+}$  ( $\text{L}=\text{dppp}$ ) is provided in Table S3 and reveals the presence of a large number of minor fragments resulting from loss of  $(\text{C}_6\text{H}_5)$  from larger primary product ions. The relative abundance of the various fragment ions is also different for clusters capped with the dcpp and dppp ligands. Although  $\text{AuL}^+$  is by far the dominant fragment for the dcpp-capped  $\text{Au}_6\text{L}_3^{2+}$  cluster, it is only a minor fragment in the spectrum of the analogous dppp-ligated cluster. In contrast,  $\text{Au}_3\text{L}^+$  is the dominant fragment ion in the spectrum of the cluster ligated with dppp as shown in Figure 4b. It is worth noting that previous studies of the dissociation of  $\text{Au}_6\text{L}_3^{2+}$  clusters capped with phenyl-substituted ligands containing between four and six carbon atoms in the alkyl chain revealed  $\text{Au}_5\text{L}_2^+$  to be the only significant fragment ion.<sup>[24]</sup> Our results show that the shorter phenyl-substituted dppp ligand, containing three carbon atoms in the alkyl chain, results in a wider range of fragmentation products from an otherwise identical  $\text{Au}_6\text{L}_3^{2+}$  cluster. Moreover, the cyclohexane-substituted dcpp ligand produces  $\text{Au}_6\text{L}_3^{2+}$  clusters that have

a relatively simple fragmentation spectrum containing only four major product ions. Therefore, it is likely that the interaction between the gold atoms of the clusters and the  $\pi$  electrons of the phenyl rings induces more complex fragmentation for the dppp-capped clusters.

To provide an additional comparison between diphosphine ligands in a larger cluster we examined the dissociation behavior of  $\text{Au}_8\text{L}_3^{2+}$  for  $\text{L}=\text{dcpp}$  and dppp. Again, it appears that substitution of the cyclohexane groups with phenyl groups in diphosphine ligands results in a larger overall number of fragment ions, as shown in Figure 5b. In this case, an additional

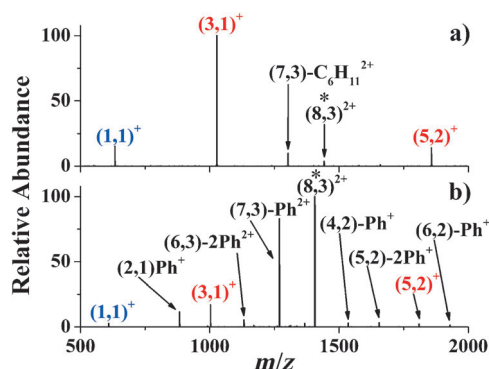


**Figure 5.** CID spectra of  $\text{Au}_8\text{L}_3^{2+}$  for (a)  $\text{L}=\text{dcpp}$  and (b)  $\text{L}=\text{dppp}$ . The isolated precursor ions are highlighted with an asterisk. The colors identify complementary fragments.

set of complementary fragment ions is observed corresponding to  $\text{Au}_2\text{L}(\text{C}_6\text{H}_5)^+$  and  $\text{Au}_6\text{L}_2-(\text{C}_6\text{H}_5)^+$  for the clusters capped with dppp that are not observed for dcpp-ligated clusters. Abundant products resulting from the loss of  $(\text{C}_6\text{H}_5)$ ,  $\text{Au}(\text{C}_6\text{H}_5)$ , and  $(\text{C}_6\text{H}_5)_2$  are also present in Figure 5b. It is noteworthy that the fragment resulting from the loss of  $\text{Au}(\text{C}_6\text{H}_{11})$  from the  $\text{Au}_8\text{L}_3^{2+}$  parent ion for dcpp-capped clusters has an analogous fragment ( $-\text{Au}(\text{C}_6\text{H}_5)$ ) for the same cluster capped with dppp. In the case of the cluster capped with dppp, however, this fragment is much more abundant. Indeed, it appears from comparison of Figure 5a and b that the large reduction in relative abundance of the complementary fragments of dppp-ligated clusters compared to clusters capped with dcpp may result from a much larger portion of the overall ion abundance being channeled into multiple fragmentation pathways that involve dissociation of the dppp ligands and loss of neutral  $\text{C}_6\text{H}_5$  and  $\text{Au}(\text{C}_6\text{H}_5)$  units.

## Conclusion

Sodium borohydride reduction of the chloro(triphenylphosphine)gold(I) precursor in the presence of dcpp in methanol/chloroform is shown to result in the preferential formation of novel multiply charged  $\text{Au}_9\text{L}_4^{3+}$ ,  $\text{Au}_{13}\text{L}_5^{3+}$ ,  $\text{Au}_6\text{L}_3^{2+}$ ,  $\text{Au}_8\text{L}_3^{2+}$ , and  $\text{Au}_{10}\text{L}_4^{2+}$  ( $\text{L}=\text{dcpp}$ ) gold cluster ions with  $\text{Au}_9\text{L}_4^{3+}$  being the dominant ion observed using mass spectrometry. CID was employed to examine the fragmentation pathways of the dcpp-capped gold clusters. The triply charged  $\text{Au}_9\text{L}_4^{3+}$  and

$\text{Au}_{13}\text{L}_5^{3+}$  clusters are demonstrated to fragment primarily into complementary pairs of doubly and singly charged product ions. The doubly charged  $\text{Au}_6\text{L}_3^{2+}$ ,  $\text{Au}_8\text{L}_3^{2+}$ , and  $\text{Au}_{10}\text{L}_4^{2+}$  clusters are demonstrated to fragment predominately into complementary pairs of singly charged ions. Additionally, higher abundances of singly and doubly charged fragment ions resulting from the loss of  $\text{Au}(\text{C}_6\text{H}_{11})$  from the precursor ions are observed for the larger  $\text{Au}_8\text{L}_3^{2+}$  and  $\text{Au}_{10}\text{L}_4^{2+}$  clusters than the smaller  $\text{Au}_6\text{L}_3^{2+}$  clusters. The fragmentation pathways of two representative doubly charged clusters,  $\text{Au}_6\text{L}_3^{2+}$  and  $\text{Au}_8\text{L}_3^{2+}$ , were compared to those of related gold clusters of the same size and charge state ligated with dppp instead of dcpp to provide insight into how substitution of the phosphine centers changes the stabilizing properties of diphosphines. Whereas gold clusters containing either ligand are found to fragment through separation into complementary singly charged ions, it is shown that clusters ligated with dppp have additional strong fragmentation channels that result from the loss of one or two gold-phenyl ( $\text{Au}(\text{C}_6\text{H}_5)$ ) units from the precursor ion. In contrast, dcpp-capped gold clusters exhibit much less efficient ligand activation, which results in the loss of  $\text{C}_6\text{H}_{11}$  units.

The results presented herein indicate that in addition to the length of the alkyl-chain spacer in diphosphine ligands, the chemical substitution of the phosphine centers also has a significant influence on the size and charge state of cationic gold clusters that are formed preferentially in solution. Moreover, it is demonstrated that relatively small changes in the substitution of the phosphine centers ( $\text{C}_6\text{H}_{11}$  versus  $\text{C}_6\text{H}_5$ ) may result in significant changes in the gas-phase fragmentation pathways of otherwise identical gold clusters. Our findings serve as a word of caution that geometrical structures as well as chemical and physical properties of ligated gold clusters calculated using simplified models of phosphine and diphosphine ligands in which computationally demanding groups such as  $\text{C}_6\text{H}_5$  and  $\text{C}_6\text{H}_{11}$  are replaced by H may not always be completely consistent with experimental observations.

## Experimental Section

### Synthesis of dcpp-ligated gold clusters

Diphosphine-ligand-capped gold clusters were synthesized in solution according to a modified version of literature procedures.<sup>[8d–15]</sup> Briefly, a gold precursor, chloro(triphenylphosphine)gold(I) (99.9% Sigma-Aldrich), was dissolved in a 1:1 mixture of methanol and chloroform (Sigma-Aldrich) to create 100 mL of a 0.1 mM solution. A bidentate capping ligand, 1,3-bis(dicyclohexylphosphino)propane (95% Sigma-Aldrich), was then added to a concentration 0.1 mM. After mixing of the gold precursor and capping ligand, a strong reducing agent, sodium borohydride (96% Sigma-Aldrich), was added to give a final solution concentration of 0.5 mM. The solution was stirred rapidly at room temperature for 3 h and placed in a dark cabinet for 3 days until it turned light purple, thereby indicating the reduction of  $\text{Au}^{\text{I}}$  and the formation of gold clusters. The nanoparticle solutions were stored in the dark at room temperature in sealed Pyrex jars. The nanoparticle solutions were diluted with methanol for use in electrospray ionization without any further purification.

## Mass spectrometry

High-resolution mass spectra ( $m/\Delta m=60\,000$ ) were obtained in the positive-ion mode using a Thermo Finnigan hybrid Linear Ion Trap (LIT)/Orbitrap (San Jose, CA) mass spectrometer calibrated using Pierce Calmix. Sample solutions were introduced into the ESI source at a flow rate of  $0.5\ \mu\text{L min}^{-1}$  using a syringe pump. The mass spectrometer conditions were as follows: capillary temperature,  $200^\circ\text{C}$ ; spray voltage, 4 kV; capillary voltage, 26 V; skimmer, 78 V; quadrupole RF amplitude, 400 V; scan range, 100–2000  $m/z$ . The potential gradient in the high-pressure source region had a minor effect on the peaks observed in the mass spectrum. Mild source conditions preserving intact diphosphine-capped gold clusters were obtained using a potential gradient of about 50 V. Charged clusters were isolated and characterized using CID employing argon as an inert collision partner followed by mass spectrometry ( $\text{MS}^2$ ). Fifty scans were averaged for each mass spectrum.

A comparison between experimentally obtained mass spectra and spectra simulated using the molecular-weight calculator program (<http://omics.pnl.gov/software/MW-Calculator.php>) for  $\text{Au}_9\text{L}_4^{3+}$  and  $\text{Au}_{13}\text{L}_5^{3+}$  is presented in the Supporting Information (Figure S1). The agreement between the experimental and simulated spectra is excellent with only minor deviations observed in the abundance of the last isotope of  $\text{Au}_9\text{L}_4^{3+}$  and the first isotope of  $\text{Au}_{13}\text{L}_5^{3+}$ , thereby allowing unambiguous assignment of the molecular formulas and ionic charge states of the dcpp-capped gold clusters.

## Acknowledgements

G.E.J. acknowledges the support of the Linus Pauling Postdoctoral Fellowship Program and the Laboratory Directed Research and Development Program at the Pacific Northwest National Laboratory (PNNL). J.L. and T.P. acknowledge support from the U.S. Department of Energy (DOE), Office of Basic Energy Sciences, and Division of Chemical Sciences, Geosciences, and Biosciences. T.P. was supported in part by the DOE's Science Undergraduate Laboratory Internship (SULI) at PNNL. The research was performed using EMSL, a national scientific user facility sponsored by the U.S. DOE of Biological and Environmental Research and located at PNNL. PNNL is operated by Battelle for the U.S. DOE.

**Keywords:** cluster compounds • gold • mass spectrometry • phosphine ligands • substituent effects

- [1] R. W. Murray, *Chem. Rev.* **2008**, *108*, 2688–2720.  
[2] a) E. S. Andreiadis, M. R. Vitale, N. Mezaillies, X. Le Goff, P. Le Floch, P. Y. Toullec, V. Michelet, *Dalton Trans.* **2010**, *39*, 10608–10616; b) J. Oliver-Meseguer, J. R. Cabrero-Antonino, I. Dominguez, A. Leyva-Perez, A. Corma, *Science* **2012**, *338*, 1452–1455; c) W. E. Kaden, T. P. Wu, W. A. Kunkel, S. L. Anderson, *Science* **2009**, *326*, 826–829; d) Y. Lei, F. Mehmood, S. Lee, J. Greeley, B. Lee, S. Seifert, R. E. Winans, J. W. Elam, R. J. Meyer, P. C. Redfern, D. Teschner, R. Schlogl, M. J. Pellin, L. A. Curtiss, S. Vajda, *Science* **2010**, *328*, 224–228; e) B. Yoon, H. Hakkinen, U. Land-

- man, A. S. Worz, J. M. Antonietti, S. Abbet, K. Judai, U. Heiz, *Science* **2005**, *307*, 403–407; f) S. Zhao, G. Ramakrishnan, D. Su, R. Rieger, A. Koller, A. Orlov, *Appl. Catal. B* **2011**, *104*, 239–244; g) P. C. Shen, A. Orlov, S. Zhao, *Abstr. Pap. Am. Chem. Soc.* **2011**, *242*, “389-ENVN”; h) V. Habibpour, M. Y. Song, Z. W. Wang, J. Cookson, C. M. Brown, P. T. Bishop, R. E. Palmer, *J. Phys. Chem. C* **2012**, *116*, 26295–26299.  
[3] a) R. K. Smith, S. U. Nanayakkara, G. H. Woehle, T. P. Pearl, M. M. Blake, J. E. Hutchison, P. S. Weiss, *J. Am. Chem. Soc.* **2006**, *128*, 9266–9267; b) M. Homberger, U. Simon, *Philos. Trans. R. Soc. London Ser. A* **2010**, *368*, 1405–1453.  
[4] a) Y. Ben-Amram, R. Tel-Vered, M. Riskin, Z. G. Wang, I. Willner, *Chem. Sci.* **2012**, *3*, 162–167; b) M. Riskin, R. Tel-Vered, T. Bourenko, E. Granot, I. Willner, *J. Am. Chem. Soc.* **2008**, *130*, 9726–9733.  
[5] E. C. Dreaden, M. A. El-Sayed, *Acc. Chem. Res.* **2012**, *45*, 1854–1865.  
[6] S. A. Claridge, A. W. Castleman, S. N. Khanna, C. B. Murray, A. Sen, P. S. Weiss, *ACS Nano* **2009**, *3*, 244–255.  
[7] D. G. Evans, D. M. P. Mingos, *J. Organomet. Chem.* **1985**, *295*, 389–400.  
[8] a) J. W. Hudgens, J. M. Pettibone, T. P. Senftle, R. N. Bratton, *Inorg. Chem.* **2011**, *50*, 10178–10189; b) J. M. Pettibone, J. W. Hudgens, *Phys. Chem. Chem. Phys.* **2012**, *14*, 4142–4154; c) Y. Shichibu, K. Konishi, *Small* **2010**, *6*, 1216–1220; d) J. M. Pettibone, J. W. Hudgens, *J. Phys. Chem. Lett.* **2010**, *1*, 2536–2540.  
[9] a) R. C. Jin, H. F. Qian, Z. K. Wu, Y. Zhu, M. Z. Zhu, A. Mohanty, N. Garg, *J. Phys. Chem. Lett.* **2010**, *1*, 2903–2910; b) R. L. Wolfe, R. W. Murray, *Anal. Chem.* **2006**, *78*, 1167–1173.  
[10] K. Kimura, N. Sugimoto, S. Sato, H. Yao, Y. Negishi, T. Tsukuda, *J. Phys. Chem. C* **2009**, *113*, 14076–14082.  
[11] Y. Levi-Kalishman, P. D. Jadzinsky, N. Kalisman, H. Tsunoyama, T. Tsukuda, D. A. Bushnell, R. D. Kornberg, *J. Am. Chem. Soc.* **2011**, *133*, 2976–2982.  
[12] D. H. Tsai, T. J. Cho, F. W. DelRio, J. Taurozzi, M. R. Zachariah, V. A. Hackley, *J. Am. Chem. Soc.* **2011**, *133*, 8884–8887.  
[13] S. Knoppe, J. Boudon, I. Dolamic, A. Dass, T. Burgi, *Anal. Chem.* **2011**, *83*, 5056–5061.  
[14] a) J. M. Pettibone, J. W. Hudgens, *ACS Nano* **2011**, *5*, 2989–3002; b) J. M. M. Smits, J. J. Bour, F. A. Vollenbroek, P. T. Beurskens, *J. Cryst. Spectrosc.* **1983**, *13*, 355–363.  
[15] M. F. Bertino, Z. M. Sun, R. Zhang, L. S. Wang, *J. Phys. Chem. B* **2006**, *110*, 21416–21418.  
[16] D. E. Bergeron, J. W. Hudgens, *J. Phys. Chem. C* **2007**, *111*, 8195–8201.  
[17] D. E. Bergeron, O. Coskuner, J. W. Hudgens, C. A. Gonzalez, *J. Phys. Chem. C* **2008**, *112*, 12808–12814.  
[18] J. M. Pettibone, J. W. Hudgens, *Small* **2012**, *8*, 715–725.  
[19] S. Hong, G. Shafai, M. Bertino, T. S. Rahman, *J. Phys. Chem. C* **2011**, *115*, 14478–14487.  
[20] J. S. Golightly, L. Gao, A. W. Castleman, D. E. Bergeron, J. W. Hudgens, R. J. Magyar, C. A. Gonzalez, *J. Phys. Chem. C* **2007**, *111*, 14625–14627.  
[21] G. E. Johnson, C. Wang, T. Priest, J. Laskin, *Anal. Chem.* **2011**, *83*, 8069–8072.  
[22] a) M. Brack, *Rev. Mod. Phys.* **1993**, *65*, 677–732; b) W. A. de Heer, *Rev. Mod. Phys.* **1993**, *65*, 611–676.  
[23] a) B. S. Gutrath, I. M. Oppel, O. Presly, I. Beljakov, V. Meded, W. Wenzel, U. Simon, *Angew. Chem.* **2013**, *125*, 3614–3617; b) M. Walter, P. Fronde-lius, K. Honkala, H. Hakkinen, *Phys. Rev. Lett.* **2007**, *99*, 096102.  
[24] P. S. D. Robinson, T. L. Nguyen, H. Lioe, R. A. O. J. 'O'Hair, G. N. Khairallah, *Int. J. Mass Spectrom.* **2012**, *330*, 109–117.  
[25] a) H. Schwarz, *Angew. Chem.* **2003**, *115*, 4580–4593; *Angew. Chem. Int. Ed.* **2003**, *42*, 4442–4454; b) D. Schroeder, J. Hrusak, R. H. Hertwig, W. Koch, P. Schwerdtfeger, H. Schwarz, *Organometallics* **1995**, *14*, 312–316.

Received: April 17, 2013

Published online on June 28, 2013



This paper is part of a Special Issue dedicated to the memory of Detlef Schröder. To view the complete issue, visit: <http://onlinelibrary.wiley.com/doi/10.1002/cplu.v78.9/issuetoc>